American Mineralogist, Volume 92, pages 1610–1615, 2007

# Pressure-induced over-hydration of thomsonite: A synchrotron powder diffraction study

Anna Yu. Likhacheva,[1,*] Yuriy V. Seryotkin,[1] Andrey Yu. Manakov,[2] Sergey V. Goryainov,[1] Aleksey I. Ancharov,[3] and Mikhail A. Sheromov[4]

[1]Institute of Geology and Mineralogy SibD RAS, pr.ak.Koptyuga 3, 630090 Novosibirsk, Russia
[2]Institute of Inorganic Chemistry SibD RAS, ac.Lavrentieva av. 3, 630090 Novosibirsk, Russia
[3]Institute of Solid State Chemistry SibD RAS, Kutateladze st. 18, 630218 Novosibirsk, Russia
[4]Budker Institute of Nuclear Physics SibD RAS, ac.Lavrentieva av. 11, 630090 Novosibirsk, Russia

## Abstract

The structural behavior of thomsonite compressed in aqueous medium up to 3 GPa was studied by means of in situ synchrotron powder diffraction with a diamond anvil cell. In the range between 0.0001 and 2 GPa, the compressibility of thomsonite is markedly lower than that reported previously, where a non-penetrating medium (with only 6% $H_2O$) was used. This indicates a pressure-induced hydration (PIH), which results in the transition to an over-hydrated phase observed at 2 GPa. The structure of over-hydrated thomsonite contains one additional, half-occupied $H_2O$ position, coordinated by the calcium at the Ca2 site, with a scolecite-like coordination $[CaO_4(H_2O)_3]$. The appearance of new $H_2O$ position causes a 4.5% volume expansion through the cooperative rotation of $[T_2O_5]^{\infty}$ chains, leading to the enlargement of the cross-section of the main channels parallel to **c** axis. The observed deformation mechanism is similar to that found in high-hydrated and super-hydrated natrolite, although only a half of the channels are affected by PIH. The present data indicate that the over-hydration effect in fibrous zeolites strongly depends on the partial water pressure in compressing medium.

**Keywords:** Zeolite, thomsonite, high pressure, compressibility, phase transition, crystal structure, over-hydration

## Introduction

Recent structural studies of fibrous zeolite natrolite $Na_2Al_2Si_3O_{10}\cdot 2H_2O$ and its related analogues compressed in aqueous medium (Lee et al. 2002, 2005, 2006; Colligan et al. 2005; Seryotkin et al. 2005) have created great interest in the over-hydration phenomenon, which is characterized by expansion of the framework due to a pressure-induced penetration of additional water molecules into the channels. This gives rise to a pressure-induced hydration (PIH) state of zeolite (Lee et al. 2004). Such an "anomalous" expansion is possible due to a high flexibility of the framework of fibrous zeolites provided by mutual rotation of the chains $[(Al,Si)_5O_{10}]^{\infty}$ (Baur et al. 1990). The over-hydration and associated expansion of the channels may dramatically alter the ion-exchange and other sorption properties of zeolites, offering an enormous potential for their various industrial applications. Although this unique phenomenon has been known for a relatively long time (Kholdeev et al. 1987; Belitsky et al. 1992; Moroz et al. 2001), only recently has a detailed structural study of PIH in natrolite been reported (Lee et al. 2002, 2005; Colligan et al. 2005; Seryotkin et al. 2005). The transformation to high-hydrated phase at 1 GPa is related to the appearance of new water positions in the framework channels of natrolite.

Thomsonite, $NaCa_2Al_5Si_5O_{20}\cdot 6H_2O$, is a widespread fibrous zeolite with the framework built up by $[(Al,Si)_5O_{10}]^{\infty}$-chains, similar to those in natrolite but having a different connectivity (Smith 1983; Armbruster and Gunter 2001). In thomsonite, Ca, Na and $H_2O$ reside in the major 8-ring channels that run along [001]. Two channel types with different cation arrangement can be distinguished. In the first channel type, there is a fully occupied Ca/Na1 site with either Na or Ca in equal amounts. In the center of the second channel, Ca occupies a split Ca2 position about 0.5 Å apart, which can only be 50% occupied. Of the four $H_2O$ sites, two are located in the first channel, and the other two are close to the second channel edge (Alberti et al. 1981; Stahl et al. 1990). Since thomsonite is closely related to natrolite, its structural response under compression in aqueous medium would provide a deeper understanding of PIH in this class of zeolites. The powder diffraction study of thomsonite compressed in "nominally penetrating medium" with about 6% of $H_2O$ (16:3:1 by volume of methanol:ethanol:water) did not show any apparent pressure-induced over-hydration effect or phase transitions up to 6 GPa (Lee et al. 2004). In other words, the mix methanol: ethanol:water = 16:3:1 behaves as a non-penetrating medium for thomsonite. However, our preliminary study of thomsonite compressed in water-rich medium shows a distinct deviation from the compression curve reported by Lee et al. (2004), and the transition to an expanded phase is observed at about 2 GPa (Likhacheva et al. 2006). Such a different behavior of thomsonite is apparently related to PIH induced by a high concentration of water in the pressure medium. This observation emphasizes the crucial importance of the $H_2O$ concentration that is needed for the PIH onset.

In this paper, we present the results of the powder diffraction

* E-mail: alih@uiggm.nsc.ru

studies of thomsonite compressed in water-rich medium up to 3 GPa. We characterize the evolution of lattice parameters of thomsonite and describe the refined crystal structure of over-hydrated thomsonite at $P > 2$ GPa. On this basis, we compare the over-hydration mechanisms in thomsonite and natrolite in terms of framework deformation and *P*-induced structural evolution.

## Experimental methods

A sample of thomsonite used in this study is from Berufjord (Iceland), with the chemical formula $Na_{4.04}Ca_{7.72}Sr_{0.32}[Al_{19.84}Si_{20.08}O_{80}]\cdot 25.69H_2O$. Quantitative chemical analysis was performed using a CAMEBAX electron microprobe, with an accelerating voltage of 20 kV and 30 nA beam current with a counting time of 10 s. The standards employed were albite (Al, Si, Na) and anorthite (Ca). The $H_2O$ content was determined by thermogravimetric analysis. The cell parameters at ambient conditions determined by Rietveld refinement are $a = 13.1026(7)$, $b = 13.0764(6)$, $c = 13.2311(5)$ Å, $V = 2266.95(17)$ Å$^3$, space group *Pncn*. The powdered sample was placed into a 400 × 100 µm gasket hole of a diamond anvil cell (DAC) and compressed up to 3 GPa. The DAC is based on a modified Mao-Bell design (Fursenko et al. 1984) and employs two diamonds with 1 mm diameter culets. To ensure the formation of over-hydrated thomsonite, we used water-rich mixtures of ethanol and water (3:1 to 1:3) as a pressure-transmitting medium. The pressure values were measured before and after the diffraction experiment from the R1 ruby fluorescence line (Mao et al. 1986) excited by a 514 nm line of an Ar laser. The powder diffraction experiments were performed at the fourth beamline of the VEPP-3 storage ring of Synchrotron centre SSRC of the Institute of nuclear physics, Novosibirsk (Ancharov et al. 2001), at a constant wavelength of 0.3675 Å. An MAR345 imaging plate detector (pixel dimension 100 µm) was used. Exposure times were 1–3 h, the sample to detector distance was 368 mm, and the focused X-ray beam was 100 × 100 µm$^2$ in size. The program FIT2D (Hammersley et al. 1996) was used for integrating the two-dimensional images up to $2\Theta_{max} = 25°$. The lattice parameters of thomsonite at different pressures were refined by whole pattern fitting using the Rietveld method, with the GSAS package (Larson and Von Dreele 2000). The diffraction patterns for the low-pressure (LP), high-pressure (HP) phase and their mixture at the transition point (at 2 GPa) are shown in Figure 1. The diffraction profiles collected at ambient pressure (hereafter 0.0001 GPa) and 2.1 GPa (Fig. 2) were used for the structure refinements.

Rietveld refinement of the crystal structure was performed using data in the 2θ range 3–25°. Because of inevitable crystallization of ice VII in a water-rich compressing medium above 2 GPa, the most intense peaks of ice VII at 2θ = 9°, 12.5° and 15.3° were excluded from the refined pattern. Note that we were able to reproduce the formation of HP phase only in the presence of ice, i.e., in the presence of excess water. Moreover, only heating at 100 °C for 1–2 h led to a complete disappearance of the LP phase peaks. The analysis of the HP-pattern indicates that the structure of the over-hydrated phase can be described in space group *Pncn*, as for the original thomsonite; however, the unit-cell volume is larger for the HP phase. The instrumental background was approximated by a Chebyshev polynomial with 15 coefficients. The Bragg peak profiles were refined by a pseudo-Voight function corrected for asymmetry. The scattering factors for calcium and sodium atoms were used to model the extra-framework species $Ca^{2+}$ and $Na^+$, respectively. To model the $H_2O$ molecules we used the scattering factor for the fluorine atom, providing a better approximation to the scattering capability of water molecule in comparison with oxygen atom, as it was shown earlier (Seryotkin et al. 2003). The Si-O and Al-O distances were restrained to 1.62(2) and 1.74(2) Å; the refined mean values were 1.628 and 1.746 Å for the LP phase and 1.620, 1.738 Å for the HP phase, respectively. The complexity of the refined structures and a relatively narrow 2θ range used did not allow us to avoid the framework restraints, although the restraining factor was set to a minimal value of 0.5. For the same reason, the displacement parameters for all atoms were fixed to an isotropic value of 0.025 and not refined. The crystal structure of natural thomsonite (Alberti et al. 1981) was used as a starting model for the refinement of the LP structure at 0.0001 GPa. For the HP structure model, we used the refined LP structure with an additional $H_2O$ position localized from a difference Fourier synthesis in the second channel. At the first stages of the refinement, the $H_2O$-$H_2O$ and $H_2O$-$O_{fram}$ distances in the second channel were restrained. In subsequent refinements, all the $H_2O$-$H_2O$ and $H_2O$-$O_{fram}$ restraints were removed. The final refined structure parameters were the atomic coordinates (for all the atoms) and the occupancy factor for all the $H_2O$ sites. On the basis of the chemical composition, the occupancies of cation positions Ca/Na1 and Ca2 were set as Ca(50%)Na(50%) and Ca(46%)Sr(4%), respectively, and were not refined.

Refinement details for the LP and HP structure of thomsonite are reported in Table 1. The refined atomic parameters for thomsonite at 0.0001 and 2 GPa are given in Tables 2, 3, and 4. The lattice parameters refined at different pressures are reported in Table 5.

## Results and discussion

### Variation of the unit-cell parameters at high pressure

The lattice parameters of thomsonite refined at 0.0001 GPa (Table 5) are in good agreement with the literature data (Alberti et al. 1981; Stahl et al. 1990). The evolution of the lattice parameters of thomsonite with pressure compared to the data of Lee et al. (2004) for the non-penetrating medium is shown in Figure 3. In the pressure range between 0.0001–2 GPa, the compressibility of thomsonite in water-rich medium is markedly lower as compared to that of the previous data. Such a low compressibility may be regarded as indirect evidence for a pressure-enhanced hydration of the framework channels. The over-hydration effect has little influence on overall structure because of the reduction of lattice parameters anisotropic (the directions **a** and **b** are more compressible than **c**, Fig. 3b), and this is similar for all fibrous natrolite-like zeolites compressed in non-penetrating medium (Gatta 2005).

As shown in Figure 3, the broken line marks the point of transition at 2 GPa, where both LP and HP phases coexist. This

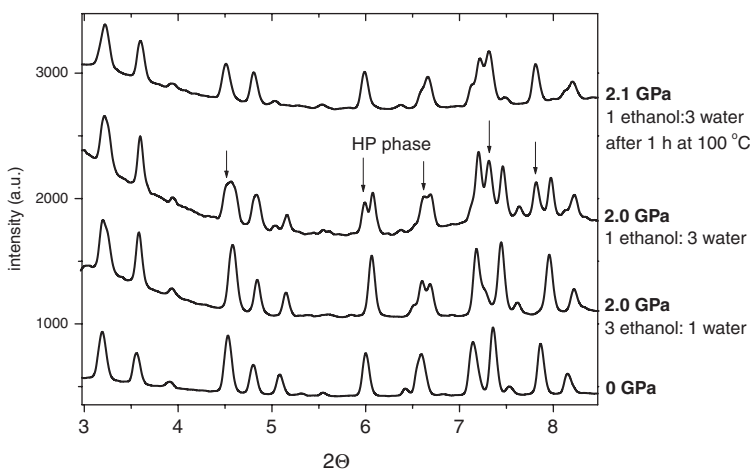


**Figure 1.** Powder diffraction patterns of thomsonite compressed with different mixtures of ethanol and water. Arrows mark the peaks of HP phase, which appears at the compression in excess water. After the heating at 100 °C (2.1 GPa), only the HP phase is present in the sample. The diffraction patterns are limited to $2\theta_{max} = 9°$ and enlarged to give a detailed picture of the changes associated with the transition to the HP phase.

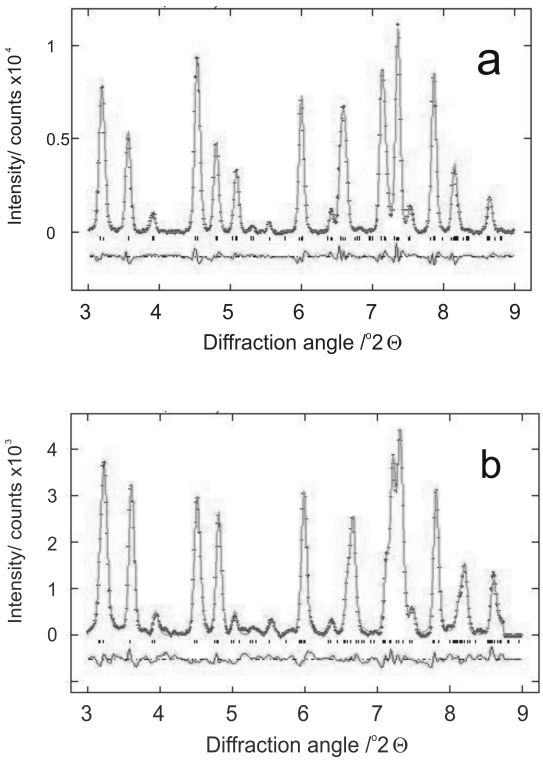


**FIGURE 2.** Results of Rietveld refinements at 0.0001 GPa (**a**) and 2.1 GPa (**b**). The observed and calculated profiles are indicated by (+) and by a continuous line, respectively. The tick marks indicate the positions of allowed Bragg peaks in the respective symmetry. A difference curve is plotted at the bottom. The part of the diffraction profile in the region of 2θ = 3–9°, shown in the figure, seems to be most "representative" because it contains all the intense reflections of thomsonite and is free from the peaks of ice VII.

**TABLE 1.** Basic crystallographic and experimental data for thomsonite at high pressures

| Pressure (GPa) | 0 | 2.1 |
|---|---|---|
| *a* (Å) | 13.1026(7) | 13.3291(9) |
| *b* (Å) | 13.0764(6) | 13.2541(10) |
| *c* (Å) | 13.2311(5) | 13.0662(7) |
| *V* (Å³) | 2266.95(17) | 2308.34(26) |
| Space group | *Pncn* | *Pncn* |
| Radiation | λ = 0.3675 Å | |
| 2θ range (°) | 3–25 | 3–25 |
| Number of observations | **2445** | **2445** |
| Number of variables | **84** | **88** |
| Number of reflections | **1798** | **1760*** |
| $R_p$ | 0.009 | 0.005 |
| $R_{wp}$ | 0.012 | 0.006 |
| $R_{F^2}$ | 0.12 | 0.15 |
| $\chi^2$ | 0.37 | 0.28 |

* The number of reflections is reduced as compared to that at 0.0001 GPa because several regions are excluded from the refinement due to the presence of ice VII.

transition is accompanied by a volume expansion of 4.5% as a result of the increase of *a* and *b* by 2.9% and 2.5%, respectively, and a compression of 0.08% along the **c** axis. Such a deformation is analogous to that observed with the formation of high-hydrated natrolite at 1.0 GPa with a 6.9% volume expansion (Lee et al. 2005; Colligan et al. 2005; Seryotkin et al. 2005), where *a* and

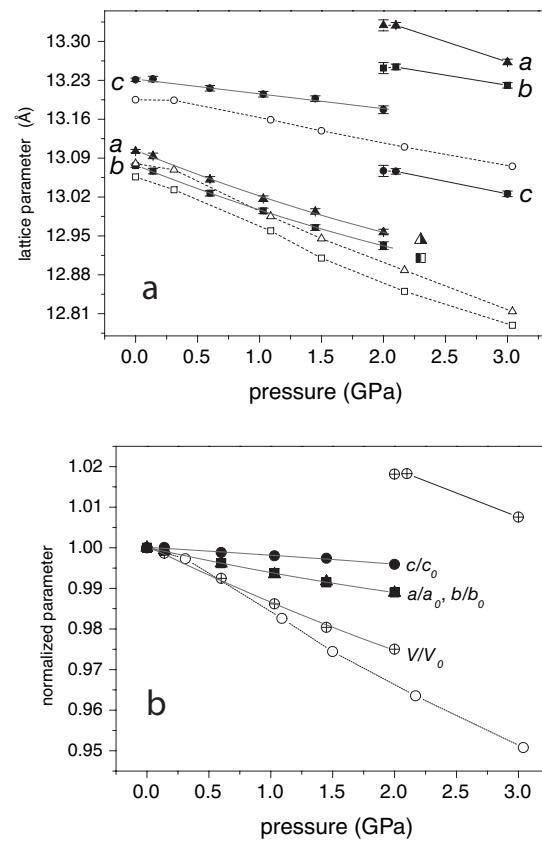


**FIGURE 3.** Pressure dependence of the lattice parameters (**a**) and normalized parameters (for LP phase) and volume (**b**) of thomsonite compressed in water-rich medium (ethanol:water ≈ 1:3, solid symbols, the data for LP phase are fitted by polynom) and in non-penetrating medium (data of Lee et al. 2004, empty symbols connected by dashed lines). Semi-filled symbols in **a** correspond to the lattice parameters of LP phase preserved at 2.3 GPa, when ethanol-rich medium (ethanol: water ≈ 3:1) was used.

*b* parameters increase by 3.3% and 3.6%, respectively. This analogy implies a similarity in structural mechanisms of the observed transitions, which, in the case of natrolite, are related to the penetration of additional $H_2O$ molecules and simultaneous enlargement of the cross-section of the main channels parallel to **c**. The deformation due to PIH in thomsonite is less dramatic with respect to that of natrolite.

It is important to note a large hysteresis and the slow kinetics of the transition observed in thomsonite, as compared to the other zeolites of the natrolite group. A mixture of the LP and HP phases occur for at least several days even at 2.4 GPa. As mentioned above, we could obtain a pure HP phase only after heating the DAC at 100 °C (2–2.4 GPa) for 1–2 h. Interestingly, we did not observe the transition to HP phase at 2–2.5 GPa when we used a mixture with the $H_2O$ content less than 50%, e.g., 3 ethanol:1 water. In this case, the diffraction pattern contains only the peaks of the LP phase with the lattice parameters close to the values at the transition point (Figs. 1 and 3a). All these features demonstrate the difficult nature of the response of thomsonite structure to PIH. This may be explained by a more close-packed

**TABLE 2.** Positional parameters for thomsonite at 0.0001 and 2.1 GPa

| Atom | *P* (GPa) | *x* | *y* | *z* | Occupancy |
|---|---|---|---|---|---|
| Ca/Na1 | 0 | 0.0595(6) | 0.5020(26) | 0.3613(4) | Ca0.5Na0.5 |
| | 2.1 | 0.0540(8) | 0.5178(12) | 0.3624(5) | Ca0.5Na0.5 |
| Ca2 | 0 | 0.4922(25) | 0.4782(9) | 0.499(4) | Ca0.46Sr0.04 |
| | 2.1 | 0.5064(26) | 0.4466(8) | 0.4903(22) | Ca0.46Sr0.04 |
| Si1 | 0 | 0.25 | 0.25 | 0.6899(5) | 1.0 |
| | 2.1 | 0.25 | 0.25 | 0.6917(5) | 1.0 |
| Al1 | 0 | 0.25 | 0.75 | 0.6914(5) | 1.0 |
| | 2.1 | 0.25 | 0.75 | 0.6904(5) | 1.0 |
| Si2 | 0 | 0.1136(5) | 0.6944(4) | 0.5002(4) | 1.0 |
| | 2.1 | 0.1165(5) | 0.6918(5) | 0.5003(4) | 1.0 |
| Al2 | 0 | 0.1199(5) | 0.3051(4) | 0.4959(4) | 1.0 |
| | 2.1 | 0.1221(5) | 0.3106(5) | 0.5005(4) | 1.0 |
| Si3 | 0 | 0.3097(4) | 0.3843(4) | 0.3816(4) | 1.0 |
| | 2.1 | 0.3037(5) | 0.3848(4) | 0.3822(4) | 1.0 |
| Al3 | 0 | 0.3121(5) | 0.6225(4) | 0.3830(4) | 1.0 |
| | 2.1 | 0.3062(5) | 0.6196(4) | 0.3837(4) | 1.0 |
| O1 | 0 | 0.1677(5) | 0.3102(7) | 0.6197(4) | 1.0 |
| | 2.1 | 0.1731(5) | 0.3155(5) | 0.6225(4) | 1.0 |
| O2 | 0 | 0.1588(5) | 0.6900(7) | 0.6157(4) | 1.0 |
| | 2.1 | 0.1622(4) | 0.6877(6) | 0.6151(4) | 1.0 |
| O3 | 0 | 0.3124(7) | 0.3323(6) | 0.7578(4) | 1.0 |
| | 2.1 | 0.3141(6) | 0.3275(5) | 0.7621(4) | 1.0 |
| O4 | 0 | 0.3112(7) | 0.6580(5) | 0.7648(4) | 1.0 |
| | 2.1 | 0.3090(6) | 0.6600(4) | 0.7666(4) | 1.0 |
| O5 | 0 | 0.0017(4) | 0.6400(7) | 0.5031(25) | 1.0 |
| | 2.1 | 0.0022(4) | 0.6510(7) | 0.4986(15) | 1.0 |
| O6 | 0 | 0.1865(5) | 0.6274(8) | 0.4258(7) | 1.0 |
| | 2.1 | 0.1830(5) | 0.6206(7) | 0.4258(6) | 1.0 |
| O7 | 0 | 0.1922(5) | 0.3865(7) | 0.4199(7) | 1.0 |
| | 2.1 | 0.1888(5) | 0.3915(6) | 0.4207(6) | 1.0 |
| O8 | 0 | 0.1020(8) | 0.8116(5) | 0.4610(7) | 1.0 |
| | 2.1 | 0.1181(7) | 0.8088(5) | 0.4646(6) | 1.0 |
| O9 | 0 | 0.1151(8) | 0.1774(5) | 0.4590(6) | 1.0 |
| | 2.1 | 0.1309(8) | 0.1865(4) | 0.4577(6) | 1.0 |
| O10 | 0 | 0.3592(7) | 0.4981(4) | 0.3828(9) | 1.0 |
| | 2.1 | 0.3523(7) | 0.4970(4) | 0.3822(8) | 1.0 |
| Ow1 | 0 | 0.1295(8) | 0.4939(28) | 0.1864(8) | 1.0 |
| | 2.1 | 0.1181(10) | 0.4891(25) | 0.1948(9) | 1.0 |
| Ow2 | 0 | 0.3905(9) | 0.500(4) | 0.6508(8) | 1.0 |
| | 2.1 | 0.4166(12) | 0.4622(13) | 0.6515(11) | 0.90(1) |
| Ow3 | 0 | 0.0 | 0.6472(16) | 0.75 | 1.0 |
| | 2.1 | 0.0 | 0.6621(20) | 0.75 | 1.0 |
| Ow4 | 0 | 0.0 | 0.3210(20) | 0.75 | 0.81(2) |
| | 2.1 | 0.0 | 0.3471(17) | 0.75 | 1.0 |
| Ow5 | 2.1 | –0.0333(27) | 0.1565(24) | 0.3435(19) | 0.51(2) |

* $U_{iso}$ for all the atoms was set to 0.025 and not refined.

**TABLE 3.** Bond distances (Å) and angles (°) for the framework tetrahedra at 0.0001 and 2.1 GPa

| Distance/angle | 0.0001 GPa | 2.1 GPa | | 0.0001 GPa | 2.1 GPa |
|---|---|---|---|---|---|
| Si1-O1 ×2 | 1.626(7) | 1.620(7) | Al1-O2 ×2 | 1.745(7) | 1.738(7) |
| Si1-O3 ×2 | 1.623(7) | 1.622(7) | Al1-O4 ×2 | 1.742(7) | 1.742(7) |
| Average | 1.625 | 1.621 | Average | 1.743 | 1.740 |
| | | | | | |
| Si2-O2 | 1.640(8) | 1.619(9) | Al2-O1 | 1.756(8) | 1.734(8) |
| Si2-O5 | 1.629(8) | 1.617(8) | Al2-O5 | 1.749(8) | 1.733(8) |
| Si2-O6 | 1.628(9) | 1.619(9) | Al2-O7 | 1.743(9) | 1.739(9) |
| Si2-O8 | 1.625(8) | 1.620(8) | Al2-O9 | 1.741(8) | 1.741(8) |
| Average | 1.630 | 1.619 | Average | 1.748 | 1.737 |
| | | | | | |
| Si3-O4 | 1.641(7) | 1.624(7) | Al3-O3 | 1.759(7) | 1.740(8) |
| Si3-O7 | 1.621(8) | 1.614(9) | Al3-O6 | 1.741(8) | 1.731(9) |
| Si3-O9 | 1.635(9) | 1.622(9) | Al3-O8 | 1.754(9) | 1.743(9) |
| Si3-O10 | 1.623(8) | 1.622(8) | Al3-O10 | 1.740(8) | 1.737(8) |
| Average | 1.629 | 1.620 | Average | 1.748 | 1.738 |
| | | | | | |
| O1-Si1-O1 | 110.4(6) | 112.1(6) | O2-Al1-O2 | 110.0(6) | 111.0(6) |
| O1-Si1-O3 ×2 | 109.2(4) | 108.1(4) | O2-Al1-O4 ×2 | 108.9(4) | 107.6(4) |
| O1-Si1-O3 ×2 | 107.6(4) | 108.8(4) | O2-Al1-O4 ×2 | 108.4(4) | 110.2(4) |
| O3-Si1-O3 | 112.8(6) | 110.9(6) | O4-Al1-O4 | 112.3(6) | 110.2(6) |
| | | | | | |
| O2-Si2-O5 | 106.7(12) | 110.8(8) | O1-Al2-O5 | 107.6(11) | 110.9(7) |
| O2-Si2-O6 | 109.4(5) | 109.4(5) | O1-Al2-O7 | 108.7(5) | 109.1(5) |
| O2-Si2-O8 | 111.4(6) | 107.1(6) | O1-Al2-O9 | 108.1(5) | 107.7(5) |
| O5-Si2-O6 | 107.9(9) | 108.3(7) | O5-Al2-O7 | 104.4(8) | 108.2(6) |
| O5-Si2-O8 | 109.6(7) | 109.1(6) | O5-Al2-O9 | 111.3(6) | 110.1(6) |
| O6-Si2-O8 | 111.6(6) | 112.1(6) | O7-Al2-O9 | 116.4(5) | 110.9(5) |
| | | | | | |
| O4-Si3-O7 | 108.2(6) | 110.6(6) | O3-Al3-O6 | 107.2(5) | 110.1(5) |
| O4-Si3-O9 | 114.6(5) | 109.2(5) | O3-Al3-O8 | 112.8(5) | 107.4(5) |
| O4-Si3-O10 | 108.3(6) | 108.5(6) | O3-Al3-O10 | 108.2(5) | 110.2(5) |
| O7-Si3-O9 | 112.6(6) | 110.7(6) | O6-Al3-O8 | 113.4(5) | 110.6(5) |
| O7-Si3-O10 | 111.1(6) | 109.2(6) | O6-Al3-O10 | 111.7(5) | 110.2(5) |
| O9-Si3-O10 | 101.8(5) | 108.6(6) | O8-Al3-O10 | 103.5(5) | 108.1(5) |
| | | | | | |
| Si1-O1-Al2 | 138.7(6) | 137.9(5) | Si2-O6-Al3 | 140.5(6) | 135.6(6) |
| Al1-O2-Si2 | 140.0(6) | 143.4(7) | Al2-O7-Si3 | 133.3(6) | 129.6(6) |
| Si1-O3-Al3 | 138.0(6) | 137.8(5) | Si2-O8-Al3 | 126.3(6) | 134.7(6) |
| Al1-O4-Si3 | 138.8(6) | 139.7(6) | Al2-O9-Si3 | 128.9(6) | 141.4(7) |
| Si2-O5-Al2 | 129.9(6) | 143.4(7) | Si3-O10-Al3 | 135.7(7) | 135.7(7) |

extra-framework species providing less free space for additional $H_2O$ molecules, as compared to more open structures of the other zeolites of the natrolite group.

After the transition at 2 GPa the compressibility parameters ($a/a_0$, $b/b_0$, $c/c_0$) become closer to that found by Lee et al. (2004) (Fig. 3a), i.e., the compressibility of the over-hydrated thomsonite slightly increases. A similar increase in compressibility was observed for natrolite at the transition to a super-hydrated phase at 1.5 GPa (Lee et al. 2002).

### Crystal structure of over-hydrated thomsonite at 2.1 GPa

In the structure of thomsonite at 0.0001 GPa, refined in this study (Fig. 4a, Tables 2–4), all the framework (Si,Al)-O distances and angles, as well as the distances in the cation polyhedra are in reasonable agreement with the literature data obtained from a single-crystal structure analysis (Alberti et al. 1981; Stahl et al. 1990). The individual atomic positions determined in this refinement differ on the average by 0.006 Å from those found by Alberti et al. (1981) and Stahl et al. (1990). The eightfold coordination of cation site Ca/Na1 includes four framework O atoms ($O_{fram}$) and four $H_2O$ molecules (Ow), with the Ca-($O_{fram}$,Ow) mean distance of 2.60 Å. The main difference with respect to the previous data are a relatively large Ca/Na1-Ow4 distance of 2.85 Å (instead of 2.58 Å) and the Ow4 occupancy factor slightly lower than 1. The discrepancy with respect to the thermogravimetric analysis, which indicates full occupancy for all the $H_2O$ sites, may be explained by the different humidity conditions during the thermogravimetric and the diffraction measurements. The cation site Ca2 in the second channel is coordinated by four framework O atoms and two $H_2O$ molecules, with a Ca-($O_{fram}$,Ow) mean distance of 2.50 Å (Fig. 5a). There is one short Ow1-Ow3 distance less than 3 Å.

Let us describe now the HP thomsonite structure refined at 2.1 GPa (Fig. 4b, Tables 2–4). As compared to the LP phase, the unit-cell volume increases by 4.5% due to the rotation of $[T_2O_5]^{\infty}$ chains leading to the increase of the ψ angle (Baur et al. 1990) from 20.3° to 22.2° (Fig. 4). There is a difference between natrolite and thomsonite in the representation of the overall chain rotation angle, ψ (Baur et al. 1990) (Fig. 4a). As a result, the expansion of the natrolite structure due to the PIH effect is characterized by a decrease of ψ (Lee et al. 2002, 2005; Colligan et al. 2005; Seryotkin et al. 2005), whereas the expansion of the thomsonite structure observed in this study is characterized by an increase of ψ. In addition, the contraction of thomsonite structure in non-penetrating medium to 2.1 GPa gives rise to a decrease of the ψ value from 20.03° to 18.5° (Lee et al. 2004). The mean

**TABLE 4.** Bond distances (Å) around the cations and water molecules at 0.0001 and 2.1 GPa

| Distance | 0.0001 GPa | 2.1 GPa | | 0.0001 GPa | 2.1 GPa |
|---|---|---|---|---|---|
| Ca/Na1-O5 | 2.711(33) | 2.600(19) | Ca2-Ca2 | 0.607(29) | 1.449(25) |
| Ca/Na1-O5 | 2.704(33) | 2.978(19) | Ca2-O8 | 2.664(24) | 2.429(26) |
| Ca/Na1-O6 | 2.487(24) | 2.345(15) | Ca2-O9 | 2.529(24) | 2.576(29) |
| Ca/Na1-O7 | 2.431(23) | 2.571(15) | Ca2-O10 | 2.34(4) | 2.580(35) |
| Ca/Na1-Ow1 | 2.491(12) | 2.381(16) | Ca2-O10 | 2.52(4) | 2.624(33) |
| Ca/Na1-Ow1 | 2.558(13) | 2.443(18) | Ca2-Ow2 | 2.43(5) | 2.433(34) |
| Ca/Na1-Ow3 | 2.566(30) | 2.893(28) | Ca2-Ow2 | 2.53(5) | 2.437(31) |
| Ca/Na1-Ow4 | 2.85(4) | 2.426(27) | Ca2-Ow5 | | 2.38(4) |
| Average Ca/Na-O | 2.583 | 2.624 | Average Ca-O | 2.513 | 2.552 |
| Average Ca/Na-Ow | 2.616 | 2.536 | Average Ca-Ow | 2.48 | 2.42 |
| Ow1-O1 | 2.760(25) | 2.85(4) | Ow2-O3 | 2.802(35) | 2.674(32) |
| Ow1-O2 | 2.603(27) | 2.63(4) | Ow2-O4 | 2.760(33) | 3.34(3) |
| Ow1-Ow3 | 2.644(30) | 2.65(4) | Ow2-O9 | >3.3 | 3.27(4) |
| Ow1-Ow4 | 3.076(24) | 2.78(4) | Ow2-O10 | 3.10(4) | 3.16(3) |
| Ow1-Ca/Na1 | 2.491(12) | 2.381(16) | Ow2-Ca2 | 2.43(5) | 2.433(34) |
| Ow1-Ca/Na1 | 2.558(13) | 2.443(18) | Ow2-Ca2 | 2.53(5) | 2.437(31) |
| | | | Ow2-Ow5 | | 2.66(4) |
| Ow3-O2 ×2 | 2.79(3) | 2.81(4) | Ow4-O1 ×2 | 2.80(4) | 2.88(4) |
| Ow3-Ow1 ×2 | 2.644(35) | 2.65(4) | Ow4-Ow1 ×2 | 3.08(3) | 2.78(4) |
| Ow3-Ow5 ×2 | | 2.73(4) | Ow4-Ca/Na1 ×2 | 2.85(4) | 2.426(27) |
| Ow3-Ca/Na1 | 2.566(30) | 2.893(28) | | | |
| Ow5-O2 | | 2.74(3) | | | |
| Ow5-O4 | | 2.55(4) | | | |
| Ow5-O8 | | 2.79(3) | | | |
| Ow5-O9 | | 2.68(3) | | | |
| Ow5-Ow2 | | 2.66(4) | | | |
| Ow5-Ow3 | | 2.73(4) | | | |
| Ow5-Ow5 | | 2.60(5) | | | |
| Ow5-Ca2 | | **2.38(4)** | | | |

**TABLE 5.** Unit-cell parameters of thomsonite (space group *Pncn*) in aqueous medium up to 3 GPa

| *P* (GPa) | *a* (Å) | *b* (Å) | *c* (Å) | *V* (Å$^3$) |
|---|---|---|---|---|
| **LP phase** | | | | |
| 0 | **13.1026(7)** | **13.0764(6)** | **13.2311(5)** | **2266.95(17)** |
| 0.14 | 13.094(2) | 13.0665(15) | 13.2323(15) | 2263.9(4) |
| 0.6 | 13.052(2) | 13.027(2) | 13.2157(15) | 2247.0(4) |
| 1.03 | 13.017(3) | 12.995(2) | 13.205(2) | 2233.6(6) |
| 1.45 | **12.994(2)** | **12.965(2)** | **13.197(2)** | **2223.3(5)** |
| 2.0 | **12.957(4)** | **12.9324(35)** | **13.177(4)** | **2208.0(8)** |
| **HP phase** | | | | |
| 2.0 | 13.329 (4) | 13.252(4) | 13.067(3) | 2308.1(10) |
| 2.1 | **13.3291(9)** | **13.2541(10)** | **13.0662(7)** | **2308.34(26)** |
| 3.0 | **13.263(2)** | **13.221(2)** | **13.0257(15)** | **2284.1(5)** |
| **LP phase, compressed in alcohol-rich medium** | | | | |
| 2.3 | 12.9427(9) | 12.9101(8) | 13.1457(6) | 2196.53(22) |

T-O-T angle between the chains in thomsonite increases from 133° to 140° at the transition to the HP phase. The rotation of the $[T_2O_5]^\infty$ chains results in an expansion of the channels in the *a*-*b* plane and a compensating decrease in the *c* parameter by 0.8%. The observed expansion is caused by the appearance of an additional $H_2O$ position Ow5 (Fig. 4b).

This new $H_2O$ position is situated in the second channel, which is similar to that observed in the structure of scolecite (Ow7 position) (Joswig et al. 1984), and in high-hydrated natrolite at 1 GPa and super-hydrated natrolite at 1.5 GPa (A position) (Lee et al. 2002, 2005; Colligan et al. 2005; Seryotkin et al. 2005). A slight shift of Ow5 from the main axis of elliptical cavity is most probably related to the short distance between Ow5 and the water position Ow3 in the neighboring channel (Fig. 5b), which creates a repulsive interaction between the O-H bonds of these two $H_2O$ molecules. The positions Ow5 and Ow2 lie at

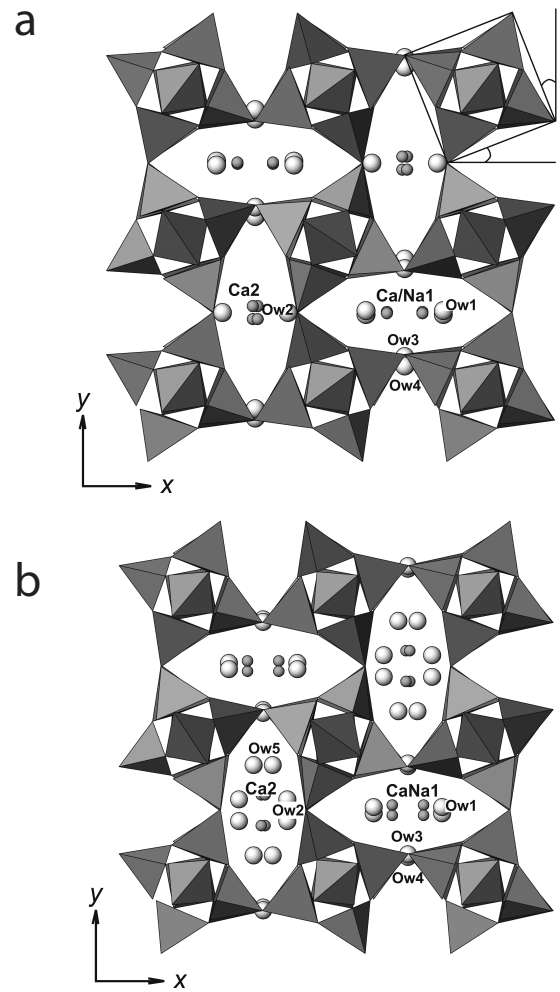


**FIGURE 4.** Crystal structure of thomsonite at 0.0001 GPa (**a**) and 2.1 GPa (HP phase) (**b**). The ψ angle of the chain rotation is shown to the right.

almost the same height along [001], which explains the shift of Ow2 away from the center of 8-membered ring (Figs. 4 and 5). Based on a half-occupied cation position Ca2, the occupancy of new position Ow5 was first set to 0.5, which was confirmed in further structure refinements. A half occupancy of Ow5 agrees with a short Ow5-Ow5 distance (Table 4), as well as with the cation-water arrangement in the second channel, where the Ca2 site is coordinated by only one Ow5 (Fig. 5b, Table 4).

Due to the appearance of new water position Ow5, the calcium coordination in the second channel changes from $O_4(H_2O)_2$ to $O_4(H_2O)_3$ (Table 4, Fig. 5). The shift of the position Ca2 out of the channel center apparently provides similar Ca-($O_{fram}$,Ow) distances in the new coordination polyhedron. The new calcium coordination may be regarded as a "scolecite-like" arrangement of the cation-water ensemble with the $H_2O$ triads displaced around the central axis of elliptical channel. As compared to the LP structure, the Ca-$O_{fram}$ distances increase and the Ca-Ow distances decrease, whereas the mean Ca-($O_{fram}$,Ow) distance in both channels remains the same despite the enlargement of the overall structure.

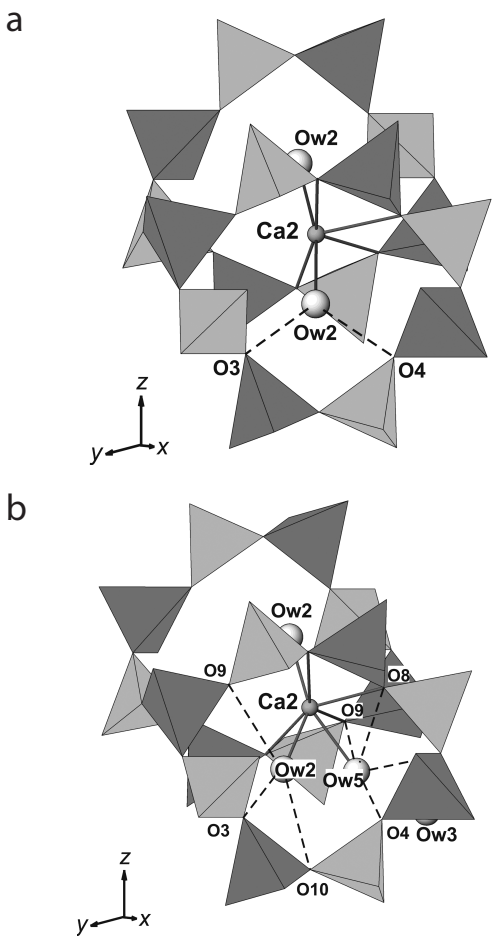


**Figure 5.** Local coordination environment of Ca2 in thomsonite (solid lines) at 0.0001 GPa (**a**) and 2.1 GPa (**b**). Dashed lines mark the short distances Ow-$O_{fram}$.

The implantation of new water position Ow5 into the second channel produces a short Ow5-Ow2 distance of 2.66 Å (Table 4, Fig. 5b). However, the direction of the vector Ow5-Ow2, if compared to those of the vectors Ca2-Ow2 and Ca2-Ow5, is not favorably oriented to form hydrogen bonds between these two $H_2O$ molecules. The angles O4-Ow5-O8 = 100° and O9-Ow2-O10 = 101° are the most appropriate with respect to the orientation of O-H vectors (Fig. 5b). Therefore, both $H_2O$ molecules are most likely linked to the framework O atoms via hydrogen bonding. The overall arrangement of the cation-water ensemble in the first channel does not change significantly with respect to the LP phase (Table 4).

## Acknowledgments

The authors are grateful to G.D. Gatta, Y. Lee, and an anonymous reviewer for their useful comments and critical reading of the manuscript. This work is supported by RFBR grant 06-05-64542, SibD RAS Integration project no. 43, and RAS Program P-9-3.

## References cited

Alberti, A., Vezzalini, G., and Tazzoli, V. (1981) Thomsonite: A detailed refinement with cross checking by crystal energy calculations. Zeolites, 1, 91–97.

Ancharov, A.I., Manakov, A.Yu., Mezentsev, N.A., Tolochko, B.P., Sheromov, M.A., and Tsukanov, V.M. (2001) New station at the 4th beamline of the VEPP-3 storage ring. Nuclear Instruments and Methods in Physics Research A, 470, 80–83.

Armbruster, Th. and Gunter, M.E. (2001) Crystal structures of natural zeolites. In D.L. Bish and D.W. Ming, Eds., Natural zeolites: Occurrence, Properties, Applications, 45, p. 1–67. Reviews in Mineralogy and Geochemistry, Mineralogical Society of America, Chantilly, Virginia.

Baur, W.H., Kassner, D., Kim, Ch.-H., and Sieber, N.H.W. (1990) Flexibility and distortion of the framework of natrolite: crystal structures of ion-exchanged natrolites. European Journal of Mineralogy, 2, 761–769.

Belitsky, I.A., Fursenko, B.A., Gabuda, S.P., Kholdeev, O.V., and Seryotkin, Yu.V. (1992) Structural transformations in natrolite and edingtonite. Physics and Chemistry of Minerals, 18, 497–505.

Colligan, M., Lee, Y., Vogt, T., Celestian, A.J., Parise, J.B., Marshall, W.G., and Hriljac, J.A. (2005) High-pressure neutron diffraction study of superhydrated natrolite. Journal of Physical Chemistry B, 109, 18223–18225.

Fursenko, B.A., Litvin, Yu.A., and Kropachev, V.D. (1984) Apparatus with transparent anvils-windows for optical and X-ray studies at high pressures. Pribory I Technika Experimenta, 174–178 (in Russian).

Gatta, G.D. (2005) A comparative study of fibrous zeolites under pressure. European Journal of Mineralogy, 17, 411–421.

Hammersley, A.P., Svensson, S.O., Hanfland, M., Fitch, A.N., and Hausermann, D. (1996) Two-dimensional detector software: from real detector to idealized image or two-theta scan. High Pressure Research, 14, 235–248.

Joswig, W., Bartl, H., and Fuess, H. (1984) Structure refinement of scolecite by neutron diffraction. Zeitschrift fur Kristallographie, 166, 219–223.

Kholdeev, O.V., Belitsky, I.A., Fursenko, B.A., and Goryainov, S.V. (1987) Structural phase transformations in natrolite at high pressure. Doklady Akademii Nauk SSSR, 297, 946–950.

Larson, A.C. and Von Dreele, R.B. (2000) General structure analysis system (GSAS). Los Alamos National Laboratory Report LAUR, 86–748.

Lee, Y., Vogt, T., Hriljac, J.A., Parise, J.B., and Artioli, G. (2002) Pressure-induced volume expansion of zeolites in the natrolite group. Journal of American Chemical Society, 124, 5466–5475.

Lee, Y., Hriljac, J.A., Studer, A., and Vogt, T. (2004) Anisotropic compression of edingtonite and thomsonite to 6 GPa at room temperature. Physics and Chemistry of Minerals, 31, 22–27.

Lee, Y., Hriljac, J.A., Parise, J.B., and Vogt, T. (2005) Pressure-induced stabilization of ordered paranatrolite: a new insight into the paranatrolite controversy. American Mineralogist, 90, 252–257.

——— (2006) Pressure-induced hydration in zeolite tetranatrolite. American Mineralogist, 91, 247–251.

Likhacheva, A.Yu., Seryotkin, Yu.V., Manakov, A.Yu., Goryainov, S.V., Ancharov, A.I., and Sheromov, M.A. (2006) Anomalous compression of scolecite and thomsonite in aqueous medium to 2 GPa. High Pressure Research, 24, 449–453.

Mao, H.K., Xu, J., and Bell, P.M. (1986) Calibration of the ruby pressure gauge to 800 kbar under quasi-hydrostatic conditions. Journal of Geophysical Research, 91, 4673–4676.

Moroz, N.K., Kholopov, E.V., Belitsky, I.A., and Fursenko, B.A. (2001) Pressure-enhanced molecular self-diffusion in microporous solids. Microporous and Mesoporous Materials, 42, 113–119.

Seryotkin, Yu.V., Joswig, W., Bakakin, V.V., Belitsky, I.A., and Fursenko, B.A. (2003) High-temperature crystal structure of wairakite. European Journal of Mineralogy, 15, 475–484.

Seryotkin, Yu.V., Bakakin, V.V., Fursenko, B.A., Belitsky, I.A., Joswig, W., and Radaelli, P.G. (2005) Structural evolution of natrolite during over-hydration: a high-pressure neutron diffraction study. European Journal of Mineralogy, 17, 305–313.

Smith, J.V. (1983) Enumeration of 4-connected 3-dimensional nets and classification of framework silicates: combination of 4-1 chain and 2D nets. Zeitschrift fur Kristallographie, 165, 191–198.

Stahl, K., Kvick, A., and Smith, J.V. (1990) Thomsonite, a neutron diffraction study at 13 K. Acta Crystallographica, C46, 1370–1373.

Manuscript received January 17, 2007
Manuscript accepted May 21, 2007
Manuscript handled by G. Diego Gatta